






Modelling internal stem damage in savanna trees: Error in aboveground biomass with terrestrial laser scanning and allometry

Jed Calvert¹  | Abbey R. Yatsko²  | Judy Bresgi¹ | Alexander W. Cheesman³  | Keith Cook¹ | James Crowe¹ | Indigo Gambold¹ | Caleb Jones¹ | Liam O'Connor¹ | Tony Peter¹ | Pedro Russell-Smith¹ | Elisha Taylor¹ | Blair Trigger¹ | Baptiste Wijas²  | Amy E. Zanne^{2,4} 

¹ArborMeta, Byron Bay, New South Wales, Australia

²Biology Department, University of Miami, Coral Gables, Florida, USA

³College of Science and Engineering, James Cook University, Cairns, Queensland, Australia

⁴Cary Institute of Ecosystem Studies, Millbrook, New York, USA

Correspondence

Abbey R. Yatsko

Email: ayatsko@miami.edu

Funding information

Maxim Foundation; Iron Range Research Station; University of Miami Biology Department; National Science Foundation Graduate Research Fellowship Program, Grant/Award Number: 1938060

Handling Editor: Abebe Ali

Abstract

1. Forests and woodlands are critical terrestrial carbon stores. Tree aboveground biomass (AGB) can be estimated using allometric models and terrestrial laser scanning (TLS). However, internal tree stem damage from biotic decay is an unresolved source of error for both TLS and allometries, with implications for accurate carbon assessment.
2. We destructively harvested 63 TLS-scanned trees in an Australian savanna, quantified internal damage in each tree by sampling cross sections at multiple heights, and modelled the effect of damage on AGB estimation for individual trees and total estimated biomass. We tested the performance of TLS AGB modelling against five allometries, applying both database and field-measured wood specific gravity. For TLS-modelled and allometric AGB estimates, we tested if tree size and level of internal stem damage contributed to AGB deviations.
3. Approximately half of the trees in the study sustained 1–10% damage by volume, which was most extensive in the base and main trunk, decreasing into the crown. On average, damaged trees had 5% internal stem damage (by volume, SD = 6.65%), with some as high as 30%. We found TLS-derived quantitative structural models (TLS-QSMs) using field-measured wood specific gravity to be most accurate in estimating total biomass ($R^2 = 0.99$, +0.59% bias). TLS-QSMs tended to overpredict AGB of large, damaged trees, and AGB estimates from allometric models were largely unaffected by internal damage. For individual trees, all methods were effective for predicting field-measured AGB ($R^2 > 0.84$) and several ASMs performed well ($\pm \sim 10\%$ bias). In the absence of local wood specific gravity calibration, a pantropical ASM was most accurate.

Jed Calvert and Abbey R. Yatsko equally contributed to this work.

This is an open access article under the terms of the [Creative Commons Attribution-NonCommercial-NoDerivs](https://creativecommons.org/licenses/by-nc-nd/4.0/) License, which permits use and distribution in any medium, provided the original work is properly cited, the use is non-commercial and no modifications or adaptations are made.

© 2024 The Author(s). *Methods in Ecology and Evolution* published by John Wiley & Sons Ltd on behalf of British Ecological Society.

4. For systems where internal stem damage is low (<10% of tree volume), TLS can be used to estimate AGB with low levels of error, however more damaged wooded ecosystems (>10%) are likely to produce inflated biomass estimates if TLS is used without calibration for damage. Internal stem damage should be quantified in ASMs and incorporated into TLS-modelled AGB calibration to avoid biomass overestimation and maintain high standards of precision in forest carbon accounting.

KEYWORDS

allometric models, forest carbon, internal tree stem damage, quantitative structural models, terrestrial laser scanning, tree aboveground biomass

1 | INTRODUCTION

Forests and woodlands are critical global carbon (C) stores, absorbing atmospheric carbon dioxide (CO₂) which is sequestered in tree biomass or passed into detrital and soil C pools (Pan et al., 2011; Pörtner et al., 2022). As the Earth's climate warms due to excess C in the atmosphere, natural C sinks such as trees are potential, yet debated, resources for mitigation (Bastin et al., 2019, but see Veldman, 2019). Globally, forest C stocks are estimated to store 861 ± 66 Pg C, more than half of which is in tropical forests (Pan et al., 2011). Global estimates of tree C are derived from a combination of earth observation (EO) datasets and local plot biomass inventories (Santoro et al., 2020; Santoro & Cartus, 2023), making it critical to accurately quantify individual tree C stored as aboveground biomass (AGB; Burt et al., 2021; Xing et al., 2019) as well as identify potential sources of error.

Internal stem damage introduces error into AGB estimates by reducing the C stored in trees (Flores-Moreno et al., 2024), and often goes unquantified; if trees are assumed to be solid structures, high levels of internal stem damage should lead to overestimated forest C. Internal stem damage, here defined as decomposition or complete removal of tree heartwood and sapwood, is hypothesized to be a natural part of some species' life history (Janzen, 1976; Ruxton, 2014). It is especially prevalent in savanna ecosystems where termites, wood-decomposing fungi and fire interact, leading to significant amounts of 'missing' biomass in living trees (Adkins, 2006; Flores-Moreno et al., 2024; N'Dri et al., 2011; Perry et al., 1985; Werner & Prior, 2007; Yatsko et al., 2024). Previous studies identified internal stem damage from single points or cross-sections near the base of trees (Apolinário & Martius, 2004; Brown et al., 1995; Eleuterio et al., 2020; Werner & Prior, 2007; Zeps et al., 2017), where microbes and termites may be entering and initiating decomposition (Adkins, 2006; Perry et al., 1985). However, it remains unexplored how internal stem damage is distributed throughout a tree, and if damage is greatest at the tree base or in the crown.

A major challenge remains for our understanding of how internal stem damage introduces error in AGB estimation at a global level, as most forest and woodland ecosystems have insufficient

data on the presence and extent of internal damage. Few studies have quantified how much internal stem damage reduces AGB, and from work in several tropical ecosystems, damage was highly variable and could affect between 7% to 36% of tree AGB (Flores-Moreno et al., 2024; Heineman et al., 2015) or up to 42% of stem volume (Monda et al., 2015). Furthermore, damage may vary within trees, and measurements throughout the tree are needed to quantify variations in its distribution. Without widely used biomass models explicitly quantifying and incorporating this source of error, there is risk for AGB overestimation for ecosystems with damaged trees.

To quantify tree AGB, allometric scaling models (ASMs) are frequently used. ASMs define relationships between tree attributes such as diameter at breast height (DBH), height, and wood specific gravity (oven dry mass/green volume [gcm⁻³]) to predict AGB. Traditionally, or in a resource-limited context, accessible tools such as DBH tapes and rangefinders can be used to measure tree DBH and height. The equations underlying ASMs are informed by destructive-harvest studies (Brown, 1997; Ketterings et al., 2001), and while ASMs are widely used to estimate forest AGB, they have several limitations. Importantly, ASMs can capture internal stem damage if underlying destructive harvest data explicitly include damaged trees (Monda et al., 2015); however most published ASMs, including those that are widely used, do not specify the presence, absence or amount of damage in the trees in their datasets (e.g. Chave et al., 2014; Paul et al., 2016). ASMs applied in ecosystems with different amounts of damage may therefore produce inaccurate AGB estimates. Additionally, while crown biomass is estimated as it scales with measurements of height and DBH, ASMs fail to capture variation in crowns and general canopy structure (Ploton et al., 2016).

Increasingly, terrestrial laser scanning (TLS) is being used to estimate forest AGB. TLS is a type of ground-based LiDAR that generates mm-resolution reconstructions of tree volumes, from the individual level (Burt et al., 2021) up to entire forest stands (Calders et al., 2015; Momo Takoudjou et al., 2018). TLS maps trees in three dimensions by emitting a laser pulse and measuring the time taken for reflected light from the tree surface to return (Lemmens, 2011). Distances are inferred from reflectance time, generating 'point clouds' that represent tree structures and can be reconstructed

into volumes via quantitative structural models (QSMs) using cylinders or surface-fitting approaches (Nölke et al., 2015; Raunonen et al., 2013). From tree QSMs, one can extract measurements such as DBH, height, and total tree volume (Demol et al., 2021). AGB can be directly derived by multiplying volumes of TLS-derived QSMs (TLS-QSMs) by wood specific gravity. Wood specific gravity can be obtained from field measurements of the sampled tree population or sourced from reference databases such as Zanne et al. (2009). Wood specific gravity values are variable within and among species and at different spatial scales, so field-measured values from a specific site are likely to be most accurate (Sæbø et al., 2022). Additionally, database wood specific gravity values are often sampled from sound, millable lumber that is not decaying, and tend to be biased toward heartwood at the tree base where sampling (i.e. increment coring) is more accessible (Wassenberg et al., 2015; Wiemann & Williamson, 2012). Taken together, AGB estimated from TLS-QSMs incorporates modelled tree volume with wood specific gravity, but still remains unable to detect the amount of internal damage present in trees (Demol et al., 2022).

The suitability of TLS for measuring tree AGB has been tested using destructive harvest studies in which living trees are scanned and destructively harvested to validate biomass estimates. Demol et al. (2022) reviewed 10 TLS destructive harvest studies, comprising 391 trees from 111 species across a global range of ecosystems, to demonstrate that TLS is an accurate tool for estimating tree AGB at large scales. However, it was noted that AGB estimations for smaller trees (<1000 kg) were inflated due to over-modelling of tree volume (Demol et al., 2022). In contrast, for larger trees (>3900 kg), Burt et al. (2021) found that TLS error did not increase with tree size. Taken together, several studies indicated that TLS has the potential to provide a less biased estimate of forest AGB at landscape scales (Demol et al., 2022) and can also be used for calibrating ASMs (Momo Takoudjou et al., 2018).

Here we carry out a destructive harvest and internal damage modelling study in Far North Queensland, Australia in a savanna woodland ecosystem with a known prevalence of internal stem damage (Flores-Moreno et al., 2024). We provide the first dataset combining modelled internal stem damage extent and distribution with field-measured, TLS-QSM and ASM AGB estimates. We sought to answer four questions: (1) How accurately do TLS-QSMs estimate AGB in comparison to allometries at the scale of individual trees and total measured biomass in a savanna where hollow trees are common? (2) Does applying field-measured or database wood specific gravity values affect TLS-QSMs and allometric AGB estimate accuracy? (3) How does internal stem damage vary throughout trees? (4) Does tree size or amount of internal stem damage predict AGB deviation? We expected TLS-QSMs to capture AGB with higher accuracy than ASMs and the application of field-measured wood specific gravity to provide AGB estimates with highest accuracy. We predicted that damage would be greatest at the tree base, that small trees would contribute disproportionately to TLS-QSM overestimates of AGB, and that high levels of damage at the tree-level would lead to greater AGB overestimates from TLS-QSMs.

2 | MATERIALS AND METHODS

2.1 | Study site

The study was carried out in October 2022 in the Iron Range (Kutini-Payamu) on Cape York Peninsula, Far North Queensland (−12.7781, 143.3199). The Iron Range is a hilly coastal region of the Australian Monsoon Tropics, 530 km northwest of Cairns, with a wet-dry tropical climate. The majority of annual rainfall (mean = 2057 mm, range = 1119–3299 mm; Australian Bureau of Meteorology, 2023) is between December and April, and mean annual temperature = 26°C with a monthly average daily temperature range between 20.6 and 30.9°C. The site is a pyrogenic savanna of *Corymbia clarksoniana* and *C. tessellaris* (Myrtaceae) open forest on metamorphic coastal ranges and is surrounded by endemic mesophyll/notophyll vine forest on metamorphic slopes and plateaus (Queensland Regional Ecosystems 3.11.5 & 3.11.1; Neldner et al., 2017). Other dominant species within the savanna include *Eucalyptus tetrodonta*, *Lophostemon suaveolens* (Myrtaceae) and *Parinari nonda* (Chrysobalanaceae), with a sparse subcanopy of *Planchonia careya* (Lecythidaceae), *Grevillea parallela* (Proteaceae) and *Acacia flavescens* (Fabaceae). We capitalized on a pre-planned tree clearance to form a firebreak on two survey areas (lower 1.84 ha, upper 0.27 ha; Figure 1). Permission for fieldwork was not required. These areas had a mean stem density of 326 trees ha^{−1} and a TLS-modelled DBH range of 1.3 to 69.7 cm (mean = 17.1 cm, standard deviation [SD] = 12.1 cm, Figure S4).

2.2 | Terrestrial laser scanning and point cloud processing

The study site overlaps with an existing long-term TLS survey area. TLS scanning was carried out for the two firebreak survey areas on 12 July 2022. One hundred and forty scans (lower survey area 111; upper survey area 29) in grid layout with 10 m spacing were collected using Riegl VZ-400i Laser Scanners (RIEGL Laser Measurement Systems, Horn, Austria) on the panoramic setting at 40 millidegrees and 1200 kHz/sec (Figure S3). All trees in the study area (including harvested and not harvested) were scanned and modelled. Due to low stem density at the long-term TLS site (326 stems/ha), this scanning design was used to minimize the effects of occlusion (partial blocking of tree stems from the scanner sensor; Wang et al., 2019). Tree point clouds were registered in RiSCAN Pro v2.14 and segmented using *treeseq* v0.2.2 (Burt et al., 2019). After segmentation, the tree point clouds were modelled using *TreeQSM* v2.4.1 (Raunonen et al., 2013) to generate cylinder models and estimate tree volume. *Optqsm* (Burt, 2023) was used to optimize tree modelling, with multiple parameters (*PatchDiam1*, *PatchDiam2Min*, *PatchDiam2Max*, *BallRad1* and *BallRad2*) assessed for each tree to identify the best model, minimizing point to cylinder distance and checking for consistency across 4 models per set of *Optqsm* parameters to obtain mean and standard deviation of volume. The minimum diameter considered was 1 cm. Georeferenced field photos

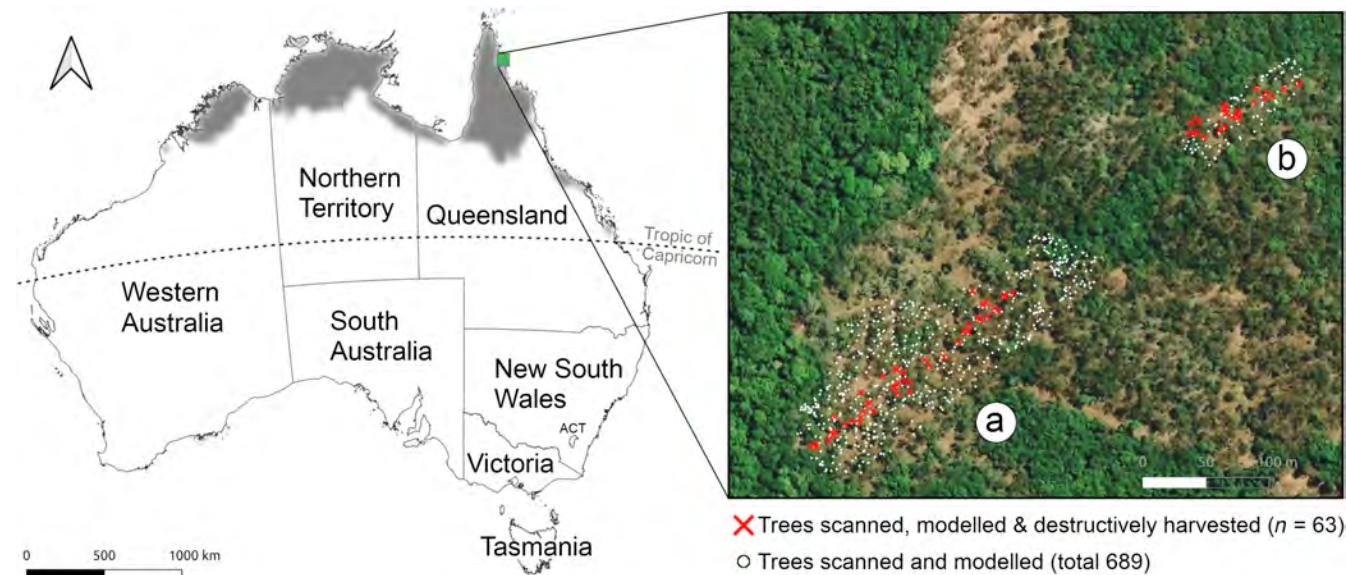


FIGURE 1 Study area. Left: Australian tropical savanna (grey, Köppen-Geiger climate classification Aw, (Beck et al., 2018) spans the northern tips of the Northern Territory, Western Australia and Queensland, where the study area is located (denoted with a green square) on Cape York Peninsula. Right: terrestrial laser scanning scan areas in lower (a) and upper (b) survey areas showing destructively harvested trees (red) and all other trees (white) that were scanned and modelled.

were used to confirm tree models. Desk audits were performed to manually check the accuracy of cylinder models against the point cloud, and poorly modelled trees were identified and reprocessed.

2.3 | Destructive harvest protocol

Sixty-three trees within the firebreak survey area were felled at ground level or, for practical reasons, at different heights up to 1 m aboveground level with a chainsaw to quantify internal stem damage and obtain field-measured biomass for each tree. Felled trees were cut into main trunk segments and crown branches for measuring field AGB within 1 h of felling using 3T (100g precision) and 250g (0.1g precision) crane scales (SCS3000, Scintex, Eagle Farm, QLD, Australia) suspended from a Manitou telehandler (Manitou Group, Ancenis, France). Trunk segments were supported for mass measurements using slings, and crown branches were weighed in a cargo net (2 × 2 m, 200 mm mesh).

2.4 | Cross-section measurements

Thirty-nine trees with signs of internal damage at the base and/or first branching point were subsampled with four to seven cross-sections distributed at heights through the stem, with the number of sections dependent on tree height to maximize the diversity of diameter size classes (Table S1, Figure 2). As trees were of different sizes and architectures, we sampled the main stem segment (cut points C1 at the felling point, C3 at the first main major branching point, and C2 midway between points C1 and C3) and then captured decreasing size classes into the crown with ascending branching orders (C4 to C7). The largest cross-sections were taken at the felling point (C1),

and the smallest in the crown branches (C7). From individual tree QSMs, we used the diameter of cross sections to determine the relative height (as a percentage) of the cross section in the tree.

Cross-sections were placed in airtight plastic bags and stored in shaded areas in the field before transport back to the laboratory. Cross-sections were then measured for green mass (m_{green}) and green volume (V_{green}) to represent field conditions. V_{green} was determined for each cross-section with the water displacement method on a balance measuring to the nearest 0.01 kg and converted to volume assuming a density of water of 1.0 g cm^{-3} . Cross-section samples were held for less than 1 week at the field station laboratory before being dried at 105°C to constant mass to determine dry mass (m_{dry}) and water content (calculated as the difference between m_{green} and m_{dry}). We calculated wood specific gravity (ρ_{wood}) for each cross-section as $m_{\text{dry}}/V_{\text{green}}$ (Panshin & De Zeeuw, 1980), which is commonly referred to as wood density in the literature (Zanne et al., 2009; Zobel & Jett, 1995).

Each cross-section was photographed to quantify the proportion of damage, measured on an area basis using a shape area classifier in Adobe Illustrator (<https://gist.github.com/bryanbuchanan/11387501>). For each photo, total proportion damage was classified as the area of damage divided by the total area of the cross-sectional sample. Total damage consisted of both microbial and termite decay (see Figure 1 in Yatsko et al. (2024) for a visual depiction of microbial and termite internal stem damage).

2.5 | Modelling tree internal damage from cross-sections

We modelled the relationship between diameter and internal damage using single-tree linear regression models for damaged trees

FIGURE 2 (a) Cross-sectional sampling from tree base to crown to quantify internal stem damage across a range of stem size classes (C1 largest, C7 smallest, see Table S1 for further detail). Note the presence of a *Coptotermes acinaciformis* mound at base, which has been linked to occurrences of high internal stem damage from field observations. This was the most internally damaged tree in the study. (b) terrestrial laser scanning point cloud of the same tree (*Corymbia clarksoniana*).

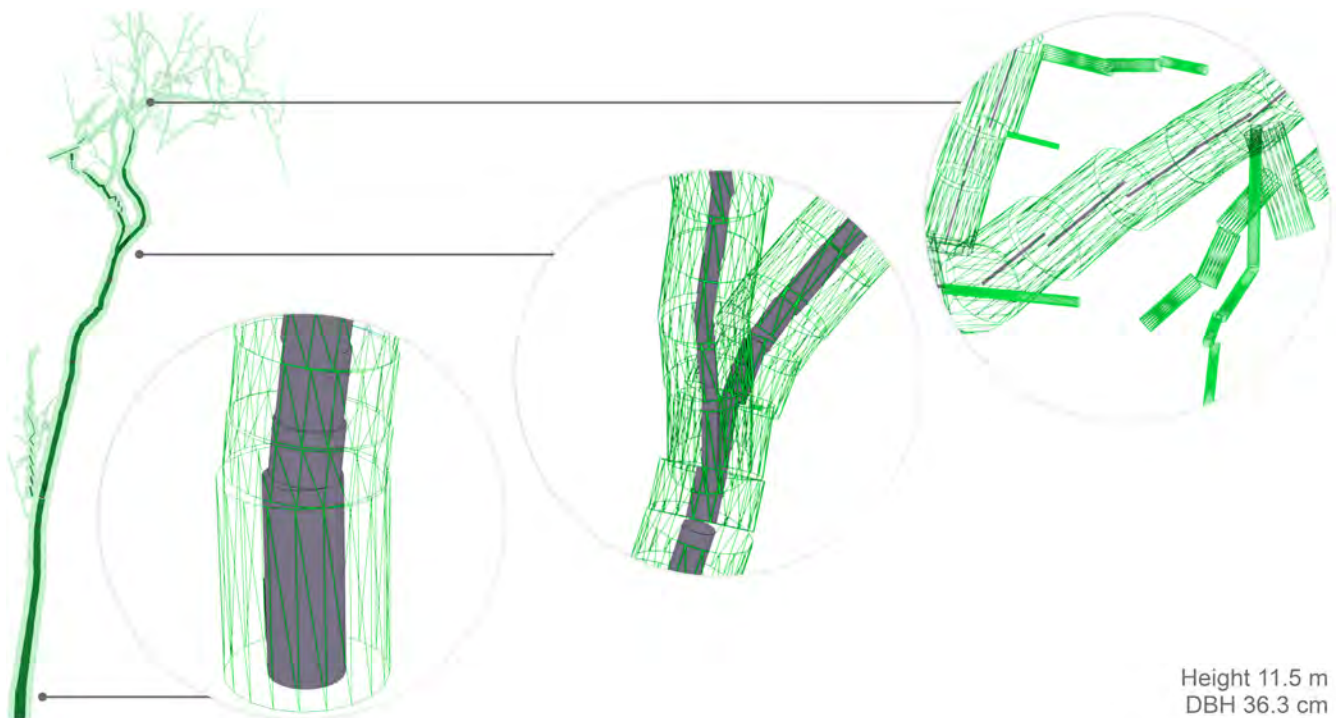
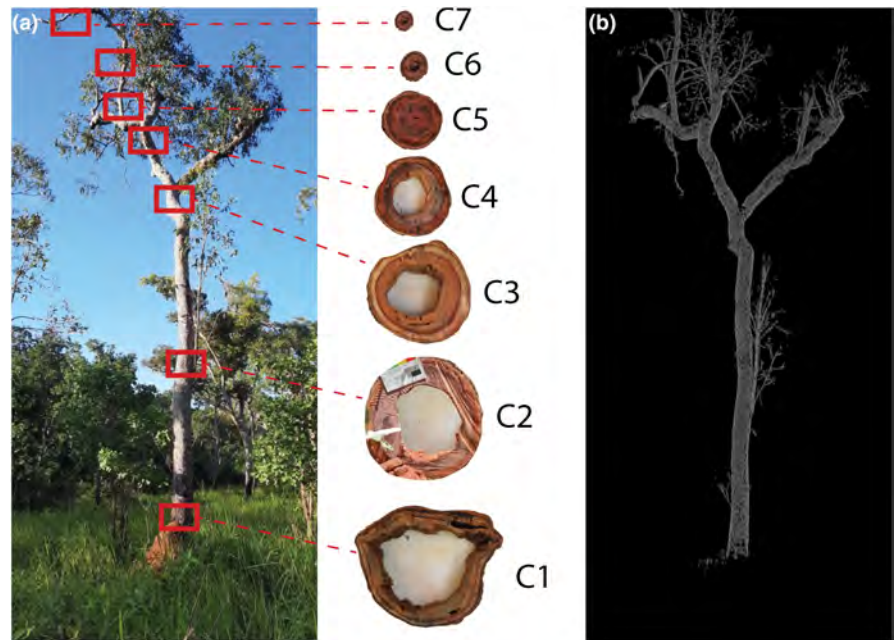


FIGURE 3 Example quantitative structural model of *Corymbia clarksoniana* (green) with internal damage modelled from linear regression (grey) for all cylinders in the model based on field observations of internal damage at cross-sections. This was the most internally damaged tree in the dataset (see Figure 2).

with ≥ 3 cross-sectional samples. We applied this tree-specific relationship of size and damage to the cylinders comprising individual tree QSMs derived from TLS (Figure 3, Table S5).

For all cylinders in the model, we calculated the average internal damage of each cylinder based on its size, and then calculated tree internal stem damage as:

$$\text{ISD}_{\text{tree}} = \int_1^C V_{\text{cyl.prop}} * \text{ISD}_{\text{lm}} \quad (1)$$

where ISD_{tree} is overall tree internal stem damage in litres (L), $V_{\text{cyl.prop}} = V_{\text{cyl}}/V_{\text{tree}}$, ISD_{lm} is internal stem damage given cylinder diameter (from individual tree-level estimate based on linear model

regression predicting internal stem damage from diameter), and C = total number of cylinders in the tree QSM.

2.6 | Species-level wood specific gravity

We examined wood specific gravity in two ways: field-measured and reference database values. For field-measured wood specific gravity, we used cross-sectional samples with no internal stem damage from different positions in the tree (Figure 2). We tested if wood specific gravity changed throughout the tree using a linear mixed effect model (R package 'lme4') with cross section diameter (in cm) and species as predictors, individual tree as a random effect, and field-measured wood specific gravity as the response variable. As cross section size had no effect on wood specific gravity (Table S10), field-measured wood specific gravity (p_{field}) at the species level was determined as average values across the undamaged cross section dataset for each species. To compare the performance of reference wood specific gravity (p_{ref}), we queried the Global Wood Density Database (Zanne et al., 2009) for values for species in our study. For trees for which species-level information was not available, we used specific gravities of closest available relatives based on molecular phylogenies (Table S2).

2.7 | Calculating AGB from TLS-QSMs

We used QSMs generated from TLS scans to determine tree volume (L), which was then multiplied by species-level p_{ref} and p_{field} to estimate AGB. All estimates in our analysis (for both TLS and ASMs discussed below) compared dry AGB, where field-measured green AGB was converted to dry AGB by multiplying m_{green} by average tree water content measured from its cross-sectional samples. We calculated TLS-estimated dry AGB for each tree by multiplying TLS-QSM tree volume (L) by wood specific gravity (for both p_{ref} and p_{field}). We define the comparison of a tree's estimated AGB with the individual tree field weight as 'tree-scale' AGB model accuracy, and the aggregated, study-wide estimated AGB versus aggregated field-weighted AGB as 'total measured biomass' AGB model accuracy.

2.8 | Calculating AGB from ASMs

To assess the performance of TLS against traditional methods of AGB estimation, we compared field-measured AGB (a physical measure of mass taken in the field) with estimates derived from five published ASMs used in tropical forest biomass literature, as well as Australian and global C markets (Table S3). The ASMs by Paul et al. (2013), later refined by Paul et al. (2016), to distinguish between eucalypts and other tree types are widely used across Australia in the Full C Accounting Method (FullCAM, Richards & Brack, 2004). Two global tropical ASMs, Brown (1997) and Chave et al. (2014), are gold-standard allometric equations for biomass,

tropical C accounting in government and voluntary C markets, and REDD+ activities (Hirata et al., 2012). Allometries from Williams et al. (2005), Paul et al. (2016), Paul et al. (2013) and Brown (1997) require DBH (here measured manually with a DBH tape) as an input to calculate AGB. The model from Chave et al. (2014) requires p_{wood} and DBH (measured manually) as inputs, which we tested using both p_{ref} and p_{field} as described above. The Chave et al. (2014) equation also includes a bioclimatic stress variable 'E', which combines temperature variability, precipitation variability and drought intensity for a given location. This value, E for the study site was determined as 0.3687456 using site latitude and longitude in the R packages 'raster' and 'ncdf4' as demonstrated in Chave et al. (2014; chave.ups-tlse.fr/pantropical_allometry.htm).

2.9 | Correcting TLS-QSM and ASM biomass for unmeasured tree stumps

For trees that were felled aboveground level ($n=38$), we corrected AGB estimates to account for the stump biomass that remained in the ground. QSMs were cut at the felling point location with a custom Python script before densities were applied to generate accurate TLS-QSM volumes (Supporting Information Data 1). ASMs for trees cut aboveground level were corrected by calculating the volume of the stump using Smalian's formula (where cylindrical volume is calculated by multiplying the average stump end area by stump height, (Köhl et al., 2006)), multiplying the resulting volume by p_{field} for a given tree and subtracting the resulting weight from the ASM weight estimate.

2.10 | Analyses

2.10.1 | Estimating AGB at the scale of individual trees and total estimated biomass with ASM and TLS

To test how well ASMs and TLS-QSMs modelled individual tree biomass before internal damage was considered, we generated linear regression models with field-measured dry AGB as the predictor and ASM/TLS-QSM biomass as the response. We compared models based on their R^2 and residual standard error (RSE) values. We evaluated how each model (five ASMs and TLS-QSM) estimated total AGB across the study area by comparing the percentage deviation from field-measured biomass for each model.

2.10.2 | Internal stem damage throughout the tree

To assess the relationship between internal stem damage and height within the tree, we used linear mixed effect models with relative height of cross section (expressed as %) in the tree and as a fixed effect, and individual tree as a random effect and percentage of internal damage as the log-transformed response.

2.10.3 | Impact of internal stem damage on AGB estimates from TLS-QSMs and ASMs

To test if TLS-QSMs and ASMs overestimated the field-measured AGB of internally damaged trees, we calculated per-tree residuals (for both TLS-QSM and the Chave et al., 2014, ASM) as TLS-QSM/ASM-predicted AGB values minus field-measured biomass and divided by field-measured biomass to normalize for tree size. We ran a linear regression with percentage of internal damage as a predictor with an interaction with DBH and residuals as the response (for both TLS-QSM and the Chave et al., 2014, ASM), expecting that if the TLS-QSM and the Chave et al., 2014, ASM overestimated true AGB, residual values would be positive. All analyses were performed in R 4.3.1 (R Core Team, 2023).

3 | RESULTS

3.1 | Estimating AGB using ASM and TLS-QSMs for individual trees

Tree AGB ranged from 2.9 kg to 3056 kg (mean = 293 kg, SD = 544 kg, Figure 4). Before modelled internal damage was considered, all ASMs and TLS-QSM gave strong predictions of field-measured AGB ($R^2 > 0.84$, Table 1) but TLS-QSMs using p_{field} provided the most precise estimates (RSE = 49.9 kg, $R^2 = 0.991$, Figure 4c, Table 1, see

Figure S1 for all comparisons). TLS-QSMs had an RSE less than half that of the best performing ASM model by Chave et al. (2014) using p_{ref} (RSE = 133.7 kg, $R^2 = 0.954$, Table 1). The ASM model from Paul et al. (2016) provided the next best prediction of field-measured AGB (RSE = 189.2 kg, $R^2 = 0.843$, Figure 4a, Table 1).

TABLE 1 Model performance for tree AGB estimates from ASMs and TLS-QSMs.

Model	p_{wood} (g cm^{-3})	R^2	Slope	Intercept	RSE (kg)
Williams 2005	n/a	0.841	1.04	23.1	246.0
Paul 2016	n/a	0.843	0.81	26.4	189.2
Paul 2013	n/a	0.844	0.63	28.1	147.6
Brown 1997	n/a	0.842	0.65	24.4	152.8
Chave 2014	Reference	0.954	1.13	1.9	133.7
Chave 2014	Field	0.914	0.97	12.6	161.7
TLS-QSM	Reference	0.974	1.11	6.5	98.8
TLS-QSM	Field	0.991	0.94	18.4	49.9

Note: Results for the Chave et al. (2014) ASM and TLS-QSMs, which both apply p_{wood} , are shown here using values published in the Global Wood Density Database (Zanne et al., 2009) (p_{ref}) as well as with field-measured species mean p_{field} .

Abbreviations: AGB, aboveground biomass; ASMs, allometric scaling models; RSE, residual standard error; TLS-QSMs, terrestrial laser scanning-quantitative structural models.

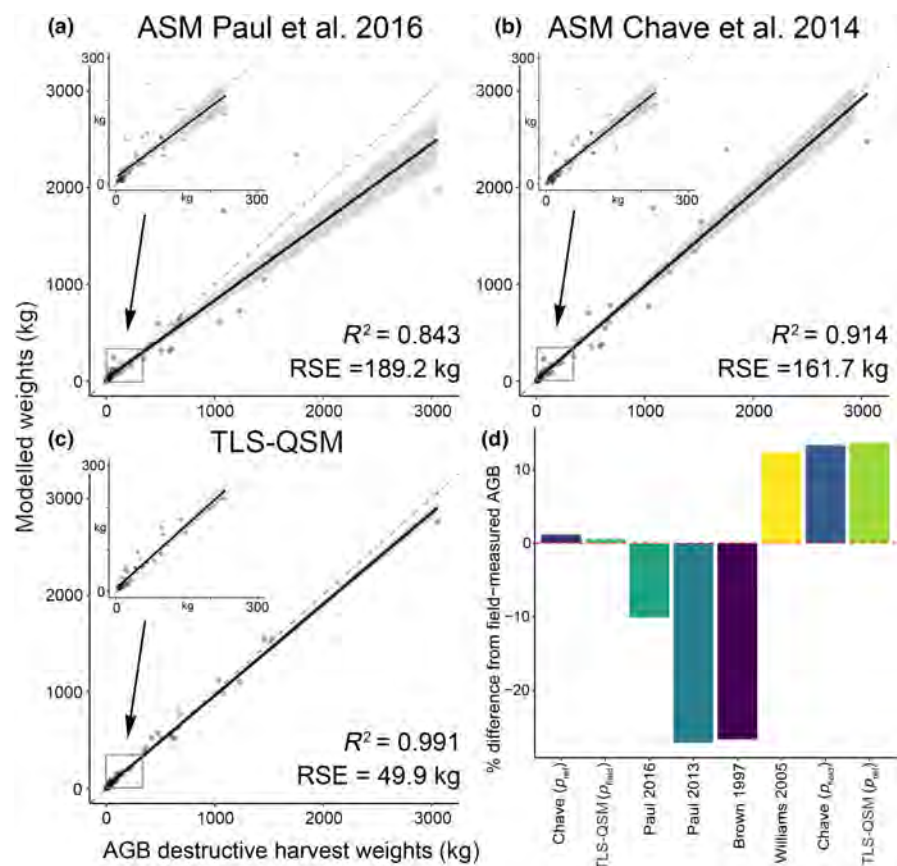


FIGURE 4 Observed aboveground biomass (AGB) from destructive harvest plotted against modelled AGB using the two highest-performing allometric scaling models (ASMs) (a: Paul et al., 2016, b: Chave et al., 2014) and AGB estimates derived from TLS-QSMs, terrestrial laser scanning-quantitative structural models (TLS-QSMs) (c). Estimates from the Chave et al. (2014) ASM (b) and TLS-QSMs (c), both use p_{field} . Grey shaded area represents a 95% confidence interval. Insets show trees <300 kg. Results for all models in Figure S1. (d) Percentage deviation from field-measured AGB for all ASMs and TLS-QSMs. Red dashed line represents field-measured AGB (baseline for comparison).

3.2 | Estimating aggregated AGB using ASMs and TLS

When we compared the sum of dry tree AGB estimates across 63 trees, the estimate closest to total field-measured AGB of destructively-harvested trees (18,438 kg) was from TLS-QSMs using p_{field} (18,546 kg, +0.59% over total field-measured AGB, Table S8). Accuracy of total measured biomass estimates from ASMs ranged from +12.3% over (Williams et al., 2005) to -27.1% under (Paul et al., 2013; Table S8, Figure 4d).

3.3 | Internal stem damage variation by species and height

Of 63 trees that were destructively harvested and modelled as QSMs, 32 trees (50.8%) had internal stem damage occurring in at least one cross-section sample. On average, damaged trees had 5% internal stem damage by volume (SD=6.65%), with some accumulating as much as 30%. Most trees had 1–10% damage by volume (94% of damaged trees, 48% of all trees). *Eucalyptus tetrodonta* trees were most frequently damaged (100%, $n=4$) while *Corymbia clarksoniana* trees had the greatest amount of internal damage (mean=7.6%, SD=8.6%, Table S6). In our mixed effect model internal stem damage significantly decreased with increasing height in damaged trees (Figure 5, $\beta=-0.02$, 95% CI [-0.03, -0.02], $t(154)=-9.48$, conditional $R^2=0.61$, marginal $R^2=0.24$, $p<0.001$). Internal damage was greatest between the base of the tree and the first branching point (Figure 5, Table S4).

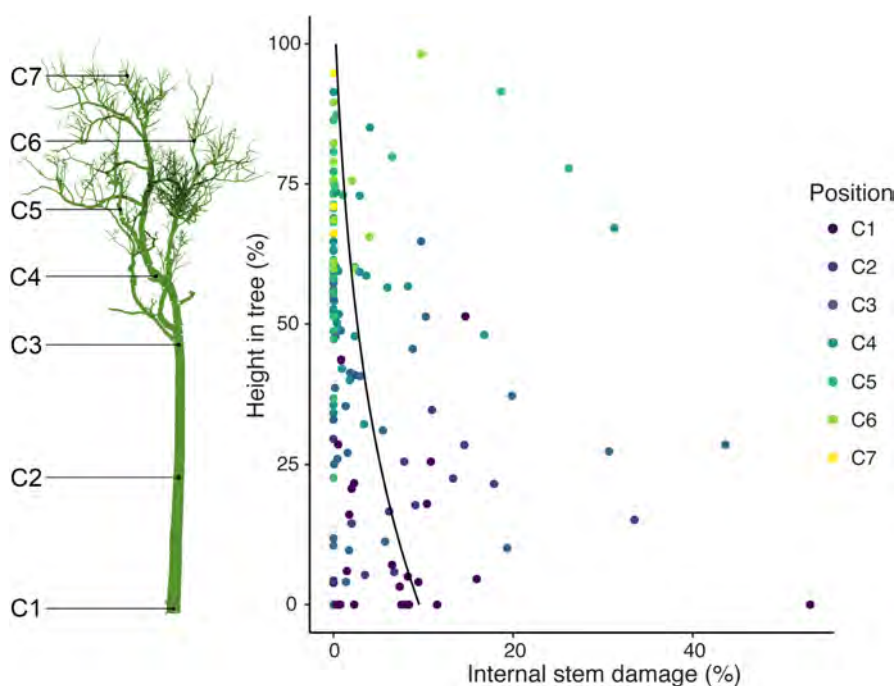


FIGURE 5 Relationship between height in tree (y-axis) and cross-sectional damage (x-axis) for all damaged trees in the study. Damage and variance are greatest toward the tree base, and less damage occurs toward the crown. Points are coloured by the position in which cross sections were taken from the tree.

3.4 | Impact of internal stem damage and tree size on AGB estimates

We found that amount of internal damage ($\beta=-0.039$, $p=0.027$) and tree DBH ($\beta=-0.014$, $p<0.001$) were significant predictors of TLS residuals, with a significant interaction between tree DBH and internal stem damage ($\beta=0.0012$, $p=0.04$, Figure 6a). Overall, TLS-QSM AGB of damaged trees was slightly overestimated, however small, damaged trees were underestimated and small, undamaged trees were overestimated (Figure S5). ASMs did not overpredict AGB for larger, damaged trees (Figure 6b).

4 | DISCUSSION

In the tropical savanna ecosystem studied here, AGB of large trees with high levels of internal damage was more likely to be overestimated by TLS-QSMs. TLS-QSMs combined with field-measured wood specific gravity best captured tree level and total measured AGB estimates, as the low levels (<10% mean by volume) of internal stem damage, which was concentrated in the lower region of the tree stem, did not have a major impact on cumulative biomass measurements. Total AGB from TLS-QSMs of all destructively-harvested trees (18.4 t) was within 0.6% of the field-measured value, a total error of 108 kg. AGB predictions from ASMs, despite being less precise than those from TLS-QSMs combined with field-measured wood specific gravity, were not significantly affected by increasing amounts of internal stem damage. It is noteworthy that in the absence of field-measured wood specific gravity (which is often the case), several of the ASMs

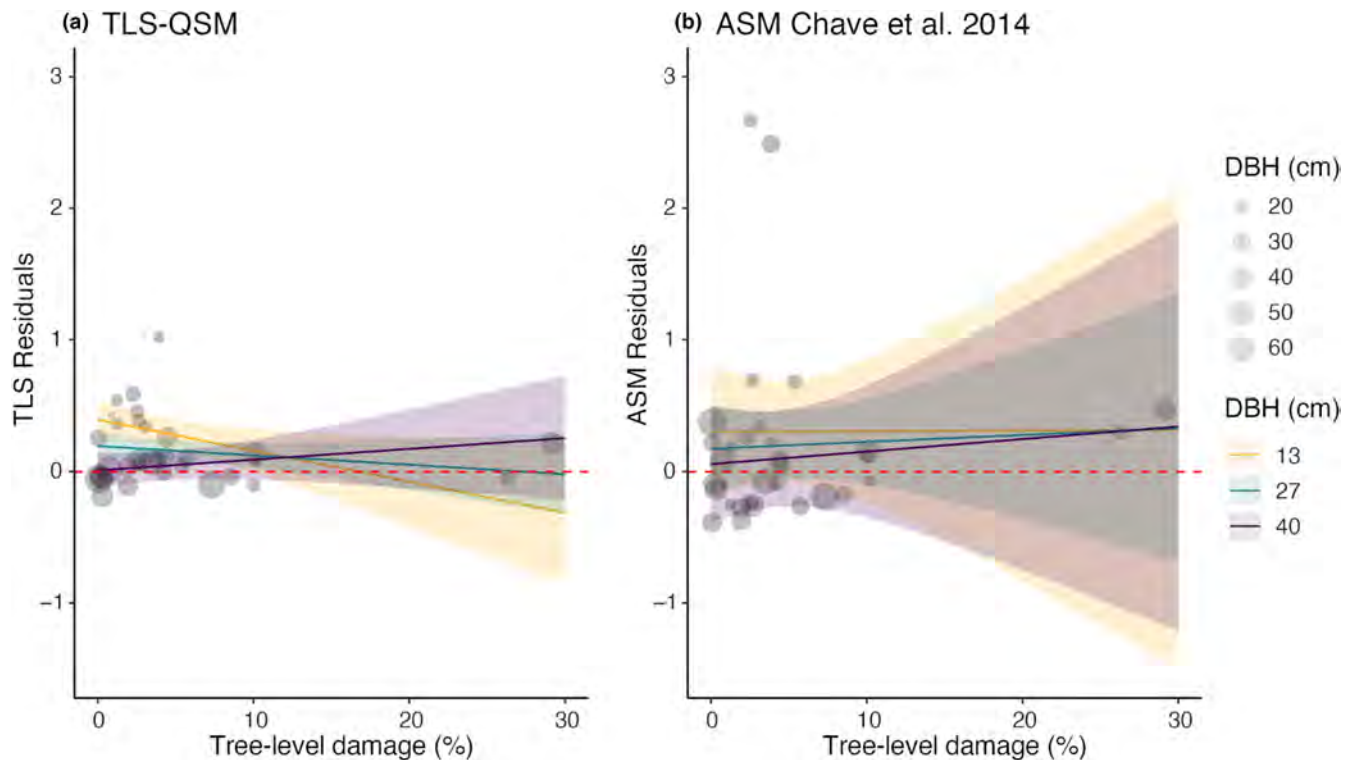


FIGURE 6 Modelled relationship between increasing internal damage (%) and normalized residuals of damaged trees (estimated aboveground biomass [AGB] [kg] minus field-measured biomass [kg], divided by tree mass [kg]). Points above the red dashed line are overestimates of AGB, while points below are underestimates; $y=1$ corresponds to an overestimate of 100% relative to tree mass. (a) Terrestrial laser scanning residuals; (b) Chave et al. (2014) ASM (p_{field}) residuals. Point size indicates tree diameter at breast height and coloured lines indicate relationships between internal damage and residuals for small (13 cm), medium (27 cm) and large (40 cm) trees relative to the destructive harvest dataset.

tested performed better than TLS-QSMs with database wood specific gravity. Together these results show support for TLS-QSMs as a highly accurate tool for estimating both total and tree-scale AGB in this low-damage system, yet application in ecosystems with large, highly damaged trees is likely to yield C overestimation. The success of TLS-QSMs was also dependent on site-specific measurements of wood specific gravity, and ASMs produced strong results with (Chave et al., 2014) and without (Paul et al., 2016; Williams et al., 2005) database values. Below we discuss our results in relation to the application of TLS and ASM in broader applied contexts.

4.1 | Internal stem damage and tree size affected TLS AGB estimation

We expected that tree-level AGB overestimations using TLS-QSMs would result from high internal stem damage and over-modelling of small trees. In line with our first expectation, we found that for larger trees, error in TLS-QSM predicted AGB was explained by increasing levels of internal damage. In our study there were only two trees with >20% damage, and the majority of the damaged trees that we sampled had <10% internal stem damage by volume, with an average of 5%. In total, this represented 488 kg or 2.6% of biomass decomposed or completely missing from within trees at the study site. Since large trees store a disproportionate amount of C in forests (Slik

et al., 2013), capturing internal stem damage in these stems will likely have a high influence on biomass accounting. Furthermore, we show that internal damage was most extensive in the lower portion of the main stem, which has more biomass to lose compared to the fine branches of the tree crown (Calders et al., 2015). Therefore in ecosystems with high damage, it may be necessary to sample internal stem damage along the main stem with less invasive methods (such as a resistograph drill, Flores-Moreno et al., 2024) to integrate potential AGB loss when using TLS-QSMs.

We observed that many trees in the study sustained fire damage to the lower trunk, as well as the presence of termite mounds at the base of three trees, which may create favourable conditions allowing for microbial and termite entry (Adkins, 2006; Perry et al., 1985) and explain the concentration of damage in the lower main stem. A noticeable characteristic of internal termite damage was carton nest material that filled in some hollow regions, which we were unable to fully remove in our field measurements of whole tree weights. Termite carton nest is likely less dense than the wood it replaced, however this still remains as a limitation in detecting the true amount of AGB that termite hollowing removed.

AGB of small trees with low (<10%) damage tended to be overestimated by TLS-QSMs, which is congruent with findings from Demol et al. (2022) and is a documented artefact of TLS-QSMs, which can struggle to model small branches (Demol et al., 2022; Hackenberg et al., 2015; Wilkes et al., 2021), but error decreases as stem size

increases. To correct for this problem, future work should fine-tune point clouds to avoid errors that inflate small tree models. For example, centroids of beams with multiple returns from small-diameter branches can be subjected to a calibrating adjustment to more accurately fit branches after initial modelling (Wilkes et al., 2021). However, although small tree AGB was less accurately predicted by TLS-QSM, the error did not adversely affect total AGB estimates as small trees (<300 kg) represented only 11% of all measured AGB.

Despite providing less precise AGB estimations in comparison to TLS-QSM, the error associated with the ASMs tested here was not impacted by internal stem damage. This finding may be attributed to the fact that the destructive harvest data underlying ASMs would have included internally damaged trees if they were present in the ecosystem. However, apart from a subset of the trees used to generate the ASM published by Williams et al. (2005), internal stem damage was neither recorded nor quantified in any other of the tested models, meaning that the generalizability and application to ecosystems with different levels of internal stem damage remains unclear (see Table S11). Indeed, ASMs have been shown to overestimate AGB and tree volumes in high damage systems (35% AGB damaged in dry savannas, Flores-Moreno et al., 2024; 42% woody volume damaged in peat swamps, Monda et al., 2015), demonstrating the cost of failing to calibrate ASMs for damage. Better descriptions of the data underlying ASMs, especially explicitly describing inclusion of internally damaged trees, would allow those who utilize such models to make better-informed choices around whether an ASM is appropriate in a given setting.

We used a single savanna site with ~5% average damage (1–30% range, by volume) to assess the impact of this missing biomass on the accuracy of AGB estimation. This is in line with other TLS destructive harvest validation studies using a single site due to the complex fieldwork logistics involved (Burt et al., 2021; Calders et al., 2015; Lau et al., 2019; Momo Takoudjou et al., 2018; Stovall et al., 2017). However, high variability of internal stem damage has been reported across a tropical rainfall gradient in Australia (mean AGB reductions of 3–35%), with highest levels of damage in dry savanna ecosystems (Flores-Moreno et al., 2024). We emphasize that further research is warranted to understand how internal stem damage interacts with TLS-QSM AGB estimation accuracy outside the savanna system in this study. A broader understanding of how internal stem damage impacts TLS-QSM AGB estimation across a range of forest types will be imperative to establish if the effects of internal damage on LiDAR-based biomass estimation observed here continue to hold true.

Another source of error that could affect AGB estimates, which was not the main focus of this study, is biomass of foliage. Although the ASMs included here explicitly incorporate foliage, TLS-QSMs do not. Due to time and logistical constraints we did not separately quantify the proportional biomass of foliage for all trees in this study; however, for four smaller trees (DBH range=6.3–24.5 cm), we removed and measured crown leaf mass. From this small subsample (assuming a leaf relative water content of 78%, (Schmidt et al., 1999)), leaf mass was estimated to be 1–4.9% of total AGB (similar to Kuyah et al., 2013; Werner & Murphy, 2001). Smaller trees had the highest foliage proportions, which is expected in savanna ecosystems (Delitti

et al., 2006). We estimate that if 4% biomass were added to TLS-QSM AGB estimates to account for foliage, total estimated biomass error would remain under +5% of destructive harvest tree weights.

4.2 | Effect of wood specific gravity values on AGB estimates

We found that using field-measured wood specific gravities in TLS-QSMs resulted in AGB estimates closer to field-measured values. For trees in our study, p_{ref} values were generally higher than p_{field} values (Figure S2), which produced AGB overestimates when applied to TLS-QSMs. Measures of p_{field} better represented trees as they were site specific, whereas wood specific gravity databases compile values from across the globe and are therefore less representative of any given site. Database values also often include measurements from only one point on the tree and may fail to incorporate changing ratios of heartwood to sapwood with different stem sizes (Sellin, 1994; Wassenberg et al., 2015). Furthermore, wood density values can be variable both within species (Patiño et al., 2009) and within individuals for different parts of the tree (Koga & Zhang, 2004), so using a single value for the wood density of a given species from a global database is unlikely to capture the range of variation that occurs in nature. Interestingly, the Chave et al. (2014) ASM had lower error when p_{ref} was used. This may be due to differences in p_{wood} for *L. suaveolens*, among the largest trees in the study, as this species and *P. nonda* were unusual in having higher p_{field} than p_{ref} . Taken together, for LiDAR-based AGB modelling, we conclude that the best estimates (in terms of R^2 and RSE) are derived from using p_{field} ; however, p_{ref} still generated TLS-QSM AGB estimates with a useful level of accuracy, as sampling trees to obtain p_{field} values is not always feasible. However, since p_{ref} is likely the most accessible measurement of wood specific gravity, this finding underscores the importance of updating and refining nuances in variation within global wood specific gravity databases.

4.3 | Applications of TLS and ASMs for estimating AGB in a low-damage ecosystem

TLS-QSMs coupled with field-measured wood specific gravity (p_{field}) provided the most precise estimate of AGB for individual tree estimates and the most accurate aggregated AGB. The ASM developed by Chave et al. (2014), which incorporated an environmental stress variable (E) and p_{ref} as well as field-measured DBH demonstrated the highest predictive power for ASMs in terms of aggregated biomass. This model, along with the ASMs by Paul et al. (2016), Williams et al. (2005) and Chave et al. (2014) with p_{field} , were all more accurate in terms of aggregated biomass than TLS-QSM with p_{ref} , however their precision in terms of RSE was substantially lower than TLS-QSM in general. It is worth noting that the Chave et al. (2014) ASM was developed using a >4000-tree dataset that contained only a small portion of Australian trees, which contrasts with the Paul et al. (2016) ASM of >15,000 Australian trees, which was tailored to represent Australian

ecosystems, including savannas (which have damaged trees), and performed more poorly. This underscores the variability of ASMs in predicting AGB; however, for situations in which estimating aggregated AGB is the primary goal and where a high level of precision is less important, ASMs remain a functional option. In scenarios where plot-based networks (i.e. ForestGEO, [ForestPlots.net](https://www.forestplots.net)) use protocols where DBH and height are manually collected, ASMs can be easily applied to estimate AGB, although incorporating TLS-QSM into such protocols is a worthwhile investment (e.g. the Smithsonian GEO-TREES initiative). TLS-QSMs and ASMs may both estimate total AGB with high accuracy, but the application of each method depends on project goals and which resources are available (i.e. are TLS scanners accessible or only DBH tapes?). The considerably lower RSE of TLS AGB estimates is important for accurate monitoring and tracking tree growth changes over time in forests and woodlands (Sheppard et al., 2016). Also, the high frequency of disturbance (i.e. cyclones and fires) in biomass-dense tropical regions can cause considerable damage to standing AGB (Zuleta et al., 2023); the inability of ASMs to capture variation in tree crown morphology (e.g. snapped or burned trees) remains a limitation that TLS-QSM approaches can overcome (Luck et al., 2020). As governments attempt to stem the tide of ecosystem destruction and rising CO₂ emissions with emerging environmental management strategies such as carbon and biodiversity markets (Carbon Credits (Carbon Farming Initiative) Act 2011; Nature Repair Market Bill, 2023), the development of accurate, scalable tools for monitoring carbon in terrestrial ecosystems has become an urgent necessity.

By providing detailed, geolocated measurements of tree architecture, ecosystem structure, canopy cover, and other ecologically important structural attributes, a further benefit of TLS-QSMs lies in translating forest metrics to larger geographical scales in a remote sensing framework. Integrating TLS-QSMs with landscape-scale airborne laser scanning (ALS) point clouds can be used to train machine learning models to interpret patterns related to vegetation structure in satellite imagery (Francis & Law, 2022; Liao et al., 2020), broadening the scale at which high-accuracy AGB estimation can be carried out. While the deployment of LiDAR at multiple scales presents a new phase in forest science, high-quality QSMs remain heavily reliant on accurate, representative wood specific gravity datasets. Improving reference wood specific gravity databases at scale with the addition of more species and explicit incorporation of intra-tree and intra-species variation will be a necessary step toward maximizing the potential of LiDAR-based AGB estimation (Chave et al., 2014; Demol et al., 2021). Furthermore, by developing LiDAR-based morphology metrics to classify tree species or functional groups, we will be able to deepen our understanding of global forest ecosystems and integrate these insights into effective carbon and biodiversity markets.

5 | CONCLUSIONS

AGB of large trees with high levels of internal damage was more likely to be overestimated by TLS-QSMs. While the low levels of internal stem damage at our study site did not significantly alter to

AGB estimates, we show that high damage in large trees will lead to AGB overestimation from TLS-QSM methods. Several ASMs performed well (\pm ~10% bias), however it is unclear whether this level of accuracy would hold for different plant communities with higher levels of damage. Future work is needed to disentangle tree traits predicting internal damage susceptibility, how fire may promote or interact with damage, and the consequences of termite and microbial damage on carbon storage. Less invasive tools such as resistograph drills or sonic tomography can be used to estimate damage in the main stem (Flores-Moreno et al., 2024; Gilbert et al., 2016), where we have shown it is most acute. Quantifying internal stem damage in this way can determine if it is a significant source of error that should be considered in forest biomass accounting.

AUTHOR CONTRIBUTIONS

Conceptualization: Jed Calvert, Abbey R. Yatsko, Alexander W. Cheesman, Keith Cook, Baptiste Wijas and Amy E. Zanne. *Data collection:* Jed Calvert, Abbey R. Yatsko, Alexander W. Cheesman, Keith Cook, Indigo Gambold, Caleb Jones, Pedro Russell-Smith, Baptiste Wijas, Judy Bresgi and Liam O'Connor. *Data analysis:* Jed Calvert, Abbey R. Yatsko, Baptiste Wijas, James Crowe, Tony Peter, Elisha Taylor and Blair Trigger. *Writing:* Jed Calvert and Abbey R. Yatsko. *Editing and review:* all authors.

ACKNOWLEDGEMENTS

The authors thank David Fell for plant species identification, Habacuc Flores-Moreno for advice on analyses, the staff at the Iron Range Research Station for their support, and James Cook University for providing equipment and materials to assist with this study. We also thank Shaun Levick and one anonymous reviewer for their constructive feedback and valuable suggestions that greatly improved our manuscript.

FUNDING INFORMATION

This work was supported by the Iron Range Research Station, the Maxim Foundation, the University of Miami Biology Department and a National Science Foundation Graduate Research Fellowship (award #1938060).

CONFLICT OF INTEREST STATEMENT

The authors declare no conflicts of interest.

PEER REVIEW

The peer review history for this article is available at <https://www.webofscience.com/api/gateway/wos/peer-review/10.1111/2041-210X.14375>.

DATA AVAILABILITY STATEMENT

R markdown and Jupyter notebook files have been uploaded to Zenodo <https://zenodo.org/records/11223163> (Yatsko, 2024).

INCLUSION STATEMENT

Our research team involves contributors from various nations, including researchers located in the region where the investigation

was conducted. All contributors were actively involved in the initial stages of the research and study blueprint to ensure the incorporation of their broad array of viewpoints. When applicable, scholarly works authored by experts from the study region were referenced.

ORCID

Jed Calvert  <https://orcid.org/0000-0002-6511-5058>

Abbey R. Yatsko  <https://orcid.org/0000-0001-8515-7629>

Alexander W. Cheesman  <https://orcid.org/0000-0003-3931-5766>

Baptiste Wijas  <https://orcid.org/0000-0001-7895-083X>

Amy E. Zanne  <https://orcid.org/0000-0001-6379-9452>

REFERENCES

- Adkins, M. F. (2006). A burning issue: Using fire to accelerate tree hollow formation in *Eucalyptus* species. *Australian Forestry*, 69(2), 107–113. <https://doi.org/10.1080/00049158.2006.10676236>
- Apolinário, F. E., & Martius, C. (2004). Ecological role of termites (Insecta, Isoptera) in tree trunks in central Amazonian rain forests. *Forest Ecology and Management*, 194(1–3), 23–28. <https://doi.org/10.1016/j.foreco.2004.01.052>
- Australian Bureau of Meteorology. (2023). *Queensland observations*. [dataset]. <http://www.bom.gov.au/qld/observations/index.shtml?ref=hdr>
- Bastin, J.-F., Finegold, Y., Garcia, C., Mollicone, D., Rezende, M., Routh, D., Zohner, C. M., & Crowther, T. W. (2019). The global tree restoration potential. *Science*, 365(6448), 76–79. <https://doi.org/10.1126/science.aax0848>
- Beck, H. E., Zimmermann, N. E., McVicar, T. R., Vergopolan, N., Berg, A., & Wood, E. F. (2018). Present and future Köppen-Geiger climate classification maps at 1-km resolution. *Scientific Data*, 5(1), 180214. <https://doi.org/10.1038/sdata.2018.214>
- Brown, I. F., Martinelli, L. A., Thomas, W. W., Moreira, M. Z., Cid Ferreira, C. A., & Victoria, R. A. (1995). Uncertainty in the biomass of Amazonian forests: An example from Rondônia, Brazil. *Forest Ecology and Management*, 75(1–3), 175–189. [https://doi.org/10.1016/0378-1127\(94\)03512-U](https://doi.org/10.1016/0378-1127(94)03512-U)
- Brown, S. (1997). *Estimating biomass and biomass change of tropical forests: A primer*. Food & Agriculture Org.
- Burt, A. (2023). *Automatically optimise and parallelise TreeQSM*. <https://github.com/apburt/optqsm>
- Burt, A., Boni Vicari, M., Da Costa, A. C. L., Coughlin, I., Meir, P., Rowland, L., & Disney, M. (2021). New insights into large tropical tree mass and structure from direct harvest and terrestrial lidar. *Royal Society Open Science*, 8, 201458. <https://doi.org/10.1098/rsos.201458>
- Burt, A., Disney, M., & Calders, K. (2019). Extracting individual trees from lidar point clouds using treeseg. *Methods in Ecology and Evolution*, 10(3), 438–445. <https://doi.org/10.1111/2041-210X.13121>
- Calders, K., Newnham, G., Burt, A., Murphy, S., Raunonen, P., Herold, M., Culvenor, D., Avitabile, V., Disney, M., Armston, J., & Kaasalainen, M. (2015). Nondestructive estimates of above-ground biomass using terrestrial laser scanning. *Methods in Ecology and Evolution*, 6(2), 198–208. <https://doi.org/10.1111/2041-210X.12301>
- Carbon Credits (Carbon Farming Initiative) Act. (2011). <https://www.legislation.gov.au/Details/C2011A00101>
- Chave, J., Réjou-Méchain, M., Búrquez, A., Chidumayo, E., Colgan, M. S., Delitti, W. B. C., Duque, A., Eid, T., Fearnside, P. M., Goodman, R. C., Henry, M., Martínez-Yrizar, A., Mugasha, W. A., Muller-Landau, H. C., Mencuccini, M., Nelson, B. W., Ngomanda, A., Nogueira, E. M., Ortiz-Malavassi, E., ... Vieilledent, G. (2014). Improved allometric models to estimate the aboveground biomass of tropical trees. *Global Change Biology*, 20(10), 3177–3190. <https://doi.org/10.1111/gcb.12629>
- Delitti, W. B. C., Meguro, M., & Pausas, J. G. (2006). Biomass and mineral mass estimates in a “cerrado” ecosystem. *Brazilian Journal of Botany*, 29, 531–540.
- Demol, M., Calders, K., Verbeeck, H., & Gielen, B. (2021). Forest above-ground volume assessments with terrestrial laser scanning: A ground-truth validation experiment in temperate, managed forests. *Annals of Botany*, 128(6), 805–819. <https://doi.org/10.1093/aob/mcab110>
- Demol, M., Verbeeck, H., Gielen, B., Armston, J., Burt, A., Disney, M., Duncanson, L., Hackenberg, J., Kükenbrink, D., Lau, A., Ploton, P., Sewdien, A., Stovall, A., Takoudjou, S. M., Volkova, L., Weston, C., Wortel, V., & Calders, K. (2022). Estimating forest above-ground biomass with terrestrial laser scanning: Current status and future directions. *Methods in Ecology and Evolution*, 13(8), 1628–1639. <https://doi.org/10.1111/2041-210X.13906>
- Eleuterio, A. A., de Jesus, M. A., & Putz, F. E. (2020). Stem decay in live trees: Heartwood hollows and termites in five timber species in eastern Amazonia. *Forests*, 11(10), 1–12. <https://doi.org/10.3390/f11101087>
- Flores-Moreno, H., Yatsko, A. R., Cheesman, A. W., Allison, S. D., Cernusak, L. A., Cheney, R., Clement, R. A., Cooper, W., Eggleton, P., Jensen, R., Rosenfield, M., & Zanne, A. E. (2024). Shifts in internal stem damage along a tropical precipitation gradient and implications for forest biomass estimation. *New Phytologist*, 241(3), 1047–1061. <https://doi.org/10.1111/nph.19417>
- Francis, J., & Law, S. (2022). Estimating Chicago's tree cover and canopy height using multi-spectral satellite imagery (arXiv:2212.05061). *arXiv* <https://doi.org/10.48550/arXiv.2212.05061>
- Gilbert, G. S., Ballesteros, J. O., Barrios-Rodríguez, C. A., Bonadies, E. F., Cedeño-Sánchez, M. L., Fossatti-Caballero, N. J., Trejos-Rodríguez, M. M., Pérez-Suñiga, J. M., Holub-Young, K. S., Henn, L. A. W., Thompson, J. B., García-López, C. G., Romo, A. C., Johnston, D. C., Barrick, P. P., Jordan, F. A., Hershovich, S., Russo, N., Sánchez, J. D., ... Hubbell, S. P. (2016). Use of sonic tomography to detect and quantify wood decay in living trees. *Applications in Plant Sciences*, 4(12), 1600060. <https://doi.org/10.3732/apps.1600060>
- Hackenberg, J., Spiecker, H., Calders, K., Disney, M., & Raunonen, P. (2015). SimpleTree—An efficient open source tool to build tree models from TLS clouds. *Forests*, 6(11), 4245–4294. <https://doi.org/10.3390/f6114245>
- Heineman, K. D., Russo, S. E., Baillie, I. C., Mamit, J. D., Chai, P. P. K., Chai, L., Hindley, E. W., Lau, B. T., Tan, S., & Ashton, P. S. (2015). Evaluation of stem rot in 339 Bornean tree species: Implications of size, taxonomy, and soil-related variation for aboveground biomass estimates. *Biogeosciences*, 12(19), 5735–5751. <https://doi.org/10.5194/bg-12-5735-2015>
- Hirata, Y., Takao, G., Sato, T., & Toriyama, J. (2012). *REDD-plus COOKBOOK*. REDD Research and Development Center.
- Janzen, D. H. (1976). Why tropical trees have rotten cores. *Biotropica*, 8(2), 110. <https://doi.org/10.2307/2989630>
- Ketterings, Q. M., Coe, R., Van Noordwijk, M., Ambagau, Y., & Palm, C. A. (2001). Reducing uncertainty in the use of allometric biomass equations for predicting above-ground tree biomass in mixed secondary forests. *Forest Ecology and Management*, 146(1–3), 199–209. [https://doi.org/10.1016/S0378-1127\(00\)00460-6](https://doi.org/10.1016/S0378-1127(00)00460-6)
- Koga, S., & Zhang, S. Y. (2004). Inter-tree and intra-tree variations in ring width and wood density components in balsam fir (*Abies balsamea*). *Wood Science and Technology*, 38, 149–162. <https://doi.org/10.1007/s00226-004-0222-z>
- Köhl, M., Magnussen, S. S., & Marchetti, M. (2006). *Sampling methods, remote sensing and GIS multiresource forest inventory*. Springer Science & Business Media.
- Kuyah, S., Dietz, J., Muthuri, C., van Noordwijk, M., & Neufeldt, H. (2013). Allometry and partitioning of above- and below-ground biomass in farmed eucalyptus species dominant in Western Kenyan agricultural landscapes. *Biomass and Bioenergy*, 55, 276–284. <https://doi.org/10.1016/j.biombioe.2013.02.011>
- Lau, A., Calders, K., Bartholomeus, H., Martius, C., Raunonen, P., Herold, M., Vicari, M., Sukhdeo, H., Singh, J., & Goodman, R. C. (2019). Tree

- biomass equations from terrestrial LiDAR: A case study in Guyana. *Forests*, 10(6), 527. <https://doi.org/10.3390/f10060527>
- Lemmens, M. (2011). Terrestrial laser scanning. In M. Lemmens (Ed.), *Geo-information: Technologies, applications and the environment* (pp. 101–121). Springer. https://doi.org/10.1007/978-94-007-1667-4_6
- Liao, Z., van Dijk, A., He, B., Larraondo, P., & Scarth, P. (2020). Woody vegetation cover, height and biomass at 25-m resolution across Australia derived from multiple site, airborne and satellite observations. *International Journal of Applied Earth Observation and Geoinformation*, 93, 102209. <https://doi.org/10.1016/j.jag.2020.102209>
- Luck, L., Hutley, L. B., Calders, K., & Levick, S. R. (2020). Exploring the variability of tropical savanna tree structural allometry with terrestrial laser scanning. *Remote Sensing*, 12(23), 3893. <https://doi.org/10.3390/rs12233893>
- Momo Takoudjou, S., Ploton, P., Sonké, B., Hackenberg, J., Griffon, S., de Coligny, F., Kamdem, N. G., Libalah, M., Mofack, G., Le Moguédec, G., Péliissier, R., & Barbier, N. (2018). Using terrestrial laser scanning data to estimate large tropical trees biomass and calibrate allometric models: A comparison with traditional destructive approach. *Methods in Ecology and Evolution*, 9(4), 905–916. <https://doi.org/10.1111/2041-210X.12933>
- Monda, Y., Kiyono, Y., Melling, L., Damian, C., & Chaddy, A. (2015). Allometric equations considering the influence of hollow trees: A case study for tropical peat swamp forest in Sarawak. *Tropics*, 24(1), 11–22. <https://doi.org/10.3759/tropics.24.11>
- Nature Repair Market Bill. (2023). <https://www.legislation.gov.au/Details/C2023B00056>
- N'Dri, A. B., Gignoux, J., Konaté, S., Dembélé, A., & Aïdara, D. (2011). Origin of trunk damage in West African savanna trees: The interaction of fire and termites. *Journal of Tropical Ecology*, 27(3), 269–278. <https://doi.org/10.1017/S026646741000074X>
- Neldner, V., Butler, D., Guymier, G., Fensham, R., Holman, J., Cogger, H., Ford, H., Johnson, C., Holman, J., & Butler, D. (2017). *Queensland's regional ecosystems. Building and maintaining a biodiversity inventory, planning framework and information system for Queensland*. Queensland Herbarium, Department of Science, Information Technology and Innovation.
- Nölke, N., Fehrmann, L., I Nengah, S. J., Tiryana, T., Seidel, D., & Kleinn, C. (2015). On the geometry and allometry of big-buttressed trees, a challenge for forest monitoring: New insights from 3D-modeling with terrestrial laser scanning. *iForest - Biogeosciences and Forestry*, 8(5), 574–581. <https://doi.org/10.3832/ifer1449-007>
- Pan, Y., Richard, A., Pekka, E., Werner, A., Oliver, L., Simon, L., Josep, G., Robert, B., Stephen, W., & David, A. (2011). A large and persistent carbon sink in the world's forests. *Science*, 333(August), 988–993.
- Panshin, A. J., & De Zeeuw, C. (1980). *Textbook of wood technology*. Part 1. Formation, anatomy, and properties of wood.
- Patiño, S., Lloyd, J., Paiva, R., Baker, T. R., Quesada, C. A., Mercado, L. M., Schmerler, J., Schwarz, M., Santos, A. J. B., Aguilar, A., & Czimczik, C. I. (2009). Branch xylem density variations across the Amazon Basin. *Biogeosciences*, 6(4), 545–568. <https://doi.org/10.5194/bg-6-545-2009>
- Paul, K. I., Roxburgh, S. H., Chave, J., England, J. R., Zerihun, A., Specht, A., Lewis, T., Bennett, L. T., Baker, T. G., Adams, M. A., Huxtable, D., Montagu, K. D., Falster, D. S., Feller, M., Sochacki, S., Ritson, P., Bastin, G., Bartle, J., Wildy, D., ... Sinclair, J. (2016). Testing the generality of above-ground biomass allometry across plant functional types at the continent scale. *Global Change Biology*, 22(6), 2106–2124. <https://doi.org/10.1111/gcb.13201>
- Paul, K. I., Roxburgh, S. H., England, J. R., Ritson, P., Hobbs, T., Brooksbank, K., John Raison, R., Larmour, J. S., Murphy, S., Norris, J., Neumann, C., Lewis, T., Jonson, J., Carter, J. L., McArthur, G., Barton, C., & Rose, B. (2013). Development and testing of allometric equations for estimating above-ground biomass of mixed-species environmental plantings. *Forest Ecology and Management*, 310, 483–494. <https://doi.org/10.1016/j.foreco.2013.08.054>
- Perry, D. H., Lenz, M., & Watson, J. A. L. (1985). Relationships between fire, fungal rots and termite damage in Australian forest trees. *Australian Forestry*, 48(1), 46–53. <https://doi.org/10.1080/00049158.1985.10674422>
- Ploton, P., Barbier, N., Stéphane, M., Réjou-Méchain, M., Bosela, F., Chuyong, G., Dauby, G., Droissart, V., Fayolle, A., Goodman, R., Henry, M., Kamdem, N., Mukirania, J., Kenfack, D., Libalah, M., Ngomanda, A., Rossi, V., Sonké, B., Texier, N., & Péliissier, R. (2016). Closing a gap in tropical forest biomass estimation: Taking crown mass variation into account in pantropical allometries. *Biogeosciences*, 13, 1571–1585. <https://doi.org/10.5194/bg-13-1571-2016>
- Pörtner, H.-O., Roberts, D. C., Poloczanska, E. S., Mintenbeck, K., Tignor, M., Alegria, A., Craig, M., Langsdorf, S., Lösschke, S., Möller, V., & Okem, A. (2022). *IPCC, 2022: Summary for policymakers*.
- R Core Team. (2023). *R: A language and environment for statistical computing*. R Foundation for Statistical Computing.
- Raunonen, P., Kaasalainen, M., Åkerblom, M., Kaasalainen, S., Kaartinen, H., Vastaranta, M., Holopainen, M., Disney, M., & Lewis, P. (2013). Fast automatic precision tree models from terrestrial laser scanner data. *Remote Sensing*, 5, 491–520. <https://doi.org/10.3390/rs5020491>
- Richards, G., & Brack, C. (2004). A continental stock and stock change estimation approach for Australia. *Australian Forestry*, 67, 284–288. <https://doi.org/10.1080/00049158.2004.10674948>
- Ruxton, G. D. (2014). Why are so many trees hollow? *Biology Letters*, 10(11), 20140555. <https://doi.org/10.1098/rsbl.2014.0555>
- Sæbø, J. S., Socolar, J. B., Sánchez, E. P., Woodcock, P., Bousfield, C. G., Uribe, C. A. M., Edwards, D. P., & Haugaasen, T. (2022). Ignoring variation in wood density drives substantial bias in biomass estimates across spatial scales. *Environmental Research Letters*, 17(5), 054002. <https://doi.org/10.1088/1748-9326/ac62ae>
- Santoro, M., & Cartus, O. (2023). *ESA Biomass Climate Change Initiative (Biomass_cci): Global datasets of forest above-ground biomass for the years 2010, 2017, 2018, 2019 and 2020*, v4. NERC EDS Centre for Environmental Data Analysis. <https://doi.org/10.5285/af60720c1e404a9e9d2c145d2b2ead4e>
- Santoro, M., Cartus, O., Carvalhais, N., Rozendaal, D., Avitabile, V., Araza, A., De Bruin, S., Herold, M., Quegan, S., Rodríguez Veiga, P., & Balzter, H. (2020). The global forest above-ground biomass pool for 2010 estimated from high-resolution satellite observations. *Earth System Science Data Discussions*, 2020, 1–38.
- Schmidt, S., Stewart, G. R., & Ashwath, N. (1999). Monitoring plant physiological characteristics to evaluate mine site revegetation: A case study from the wet-dry tropics of northern Australia. *Plant and Soil*, 215(1), 73–84. <https://doi.org/10.1023/A:1004721330261>
- Sellin, A. (1994). Sapwood-heartwood proportion related to tree diameter, age, and growth rate in *Piceaabies*. *Canadian Journal of Forest Research*, 24(5), 1022–1028. <https://doi.org/10.1139/x94-133>
- Sheppard, J., Morhart, C., Hackenberg, J., & Spiecker, H. (2016). Terrestrial laser scanning as a tool for assessing tree growth. *iForest - Biogeosciences and Forestry*, 10, 172–197. <https://doi.org/10.3832/ifer2138-009>
- Slik, J. W. F., Paoli, G., Mcguire, K., Amaral, I., Barroso, J., Bastian, M., Blanc, L., Bongers, F., Boundja, P., Clark, C., Collins, M., Dauby, G., Ding, Y., Doucet, J. L., Eler, E., Ferreira, L., Forshed, O., Fredriksson, G., Gillet, J. F., ... Zweifel, N. (2013). Large trees drive forest above-ground biomass variation in moist lowland forests across the tropics. *Global Ecology and Biogeography*, 22(12), 1261–1271. <https://doi.org/10.1111/geb.12092>
- Stovall, A. E., Vorster, A. G., Anderson, R. S., Evangelista, P. H., & Shugart, H. H. (2017). Non-destructive aboveground biomass estimation of coniferous trees using terrestrial LiDAR. *Remote Sensing of Environment*, 200, 31–42. <https://doi.org/10.1016/j.rse.2017.08.013>
- Veldman, J. (2019). Comment on "The global tree restoration potential". *Science*, 366, 76–79. <https://www.science.org/doi/full/10.1126/science.aay7976>

- Wang, Y., Pyörälä, J., Liang, X., Lehtomäki, M., Kukko, A., Yu, X., Kaartinen, H., & Hyyppä, J. (2019). In situ biomass estimation at tree and plot levels: What did data record and what did algorithms derive from terrestrial and aerial point clouds in boreal forest. *Remote Sensing of Environment*, 232, 111309. <https://doi.org/10.1016/j.rse.2019.111309>
- Wassenberg, M., Chiu, H.-S., Guo, W., & Spiecker, H. (2015). Analysis of wood density profiles of tree stems: Incorporating vertical variations to optimize wood sampling strategies for density and biomass estimations. *Trees*, 29, 551–561. <https://doi.org/10.1007/s00468-014-1134-7>
- Werner, P. A., & Murphy, P. G. (2001). Size-specific biomass allocation and water content of above- and below-ground components of three *Eucalyptus* species in a northern Australian savanna. *Australian Journal of Botany*, 49(2), 155. <https://doi.org/10.1071/BT99026>
- Werner, P. A., & Prior, L. D. (2007). Tree-piping termites and growth and survival of host trees in savanna woodland of north Australia. *Journal of Tropical Ecology*, 23(6), 611–622. <https://doi.org/10.1017/S0266467407004476>
- Wiemann, M. C., & Williamson, G. B. (2012). *Density and specific gravity metrics in biomass research*. General Technical Report. USDA Forest Service, Forest Products Laboratory. <https://doi.org/10.2737/FPL-GTR-208>
- Wilkes, P., Shenkin, A., Disney, M., Malhi, Y., Bentley, L. P., & Vicari, M. B. (2021). Terrestrial laser scanning to reconstruct branch architecture from harvested branches. *Methods in Ecology and Evolution*, 12(12), 2487–2500. <https://doi.org/10.1111/2041-210X.13709>
- Williams, R. J., Zerihun, A., Montagu, K. D., Hoffman, M., Hutley, L. B., & Chen, X. (2005). Allometry for estimating aboveground tree biomass in tropical and subtropical eucalypt woodlands: Towards general predictive equations. *Australian Journal of Botany*, 53(7), 607. <https://doi.org/10.1071/BT04149>
- Xing, D., Bergeron, J. C., Solarik, K. A., Tomm, B., Macdonald, S. E., Spence, J. R., & He, F. (2019). Challenges in estimating forest biomass: Use of allometric equations for three boreal tree species. *Canadian Journal of Forest Research*, 49(12), 1613–1622. <https://doi.org/10.1139/cjfr-2019-0258>
- Yatsko, A. R. (2024). MEE supporting data [dataset]. Zenodo. <https://zenodo.org/records/11223163>
- Yatsko, A. R., Wijas, B., Calvert, J., Cheeseman, A. W., Cook, K., Eggleton, P., Gambold, I., Jones, C., Russell-Smith, P., & Zanne, A. E. (2024). Why are trees hollow? Termites, microbes, and tree internal stem damage in a tropical savanna. *EcoEvoRxiv* preprint <https://doi.org/10.32942/X2WG75>
- Zanne, A. E., Lopez-Gonzalez, G., Coomes, D. A., Jugo, I., Jansen, S., Lewis, S. L., Miller, R. B., Swenson, N., Wiemann, M. C., & Chave, J. (2009). Data from: Towards a worldwide wood economics spectrum. *Dryad*. <https://doi.org/10.5061/dryad.234>
- Zeps, M., Senhofa, S., Zadina, M., Neimane, U., & Jansons, A. (2017). Stem damages caused by heart rot and large poplar borer on hybrid and European aspen. *Forestry Studies*, 66, 21–26. <https://doi.org/10.1515/fsmu-2017-0003>
- Zobel, B. J., & Jett, J. B. (1995). The importance of wood density (specific gravity) and its component parts. In T. E. Timell (Ed.), *Genetics of wood production* (pp. 78–97). Springer. https://doi.org/10.1007/978-3-642-79514-5_4
- Zuleta, D., Arellano, G., McMahon, S. M., Aguilar, S., Bunyavejchewin, S., Castaño, N., Chang-Yang, C.-H., Duque, A., Mitre, D., Nasardin, M., Pérez, R., Sun, I.-F., Yao, T. L., Valencia, R., Krishna Moorthy, S. M., Verbeeck, H., & Davies, S. J. (2023). Damage to living trees contributes to almost half of the biomass losses in tropical forests. *Global Change Biology*, 29(12), 3409–3420. <https://doi.org/10.1111/gcb.16687>

SUPPORTING INFORMATION

Additional supporting information can be found online in the Supporting Information section at the end of this article.

Table S1. Sampling of tree cross-sections used in assessing internal stem damage.

Table S2. Reference wood specific gravities (Global Wood Density Database, Zanne et al., 2009) of closest available relatives from published sources for species in this study that did not have available published wood specific gravity values.

Table S3. Allometric scaling models (ASMs) that were compared with TLS-based AGB estimates.

Table S4. For damaged trees, damage frequency (%), average damage (%), and standard deviation of damage for cross sectional samples at different sampled positions across tree height.

Table S5. For damaged trees, linear regression model parameters describing relationship between internal stem damage and vertical position in the tree.

Table S6. Internal damage frequency (percentage of trees in study) and extent (mean percentage of total tree AGB and standard deviation).

Table S7. TLS and Chave 2014 ASM model performance using reference and field-measured wood specific gravity.

Table S8. Sum of observed dry tree weights, net difference from field-measured biomass (kg), and percentage difference from field-measured biomass.

Table S9. Number of individuals for each species in the study.

Table S10. Output for wood specific gravity linear mixed model for undamaged cross sections.

Table S11. Summary of how tested ASMs included or mentioned the prevalence of internally damaged trees in the underlying data from which ASMs were built.

Figure S1. Estimated and observed AGB for all ASM models tested in this study (a–f) and TLS (g, h).

Figure S2. Comparison of species mean wood specific gravities collected in this study with generalized species densities published in the Global Wood Density Database (Zanne et al., 2009).

Figure S3. Terrestrial laser scan layouts of (sites A and B).

Figure S4. (a) DBH size distribution (cm) of all trees ($n=63$) in the study and (b) DBH size distribution (cm) of damaged trees in study ($n=32$).

Figure S5. Distribution of over/underestimates of field-measured biomass from TLS (a) and Chave 2014 ASM (b) for undamaged trees, normalized by tree size.

How to cite this article: Calvert, J., Yatsko, A. R., Bresgi, J., Cheeseman, A. W., Cook, K., Crowe, J., Gambold, I., Jones, C., O'Connor, L., Peter, T., Russell-Smith, P., Taylor, E., Trigger, B., Wijas, B., & Zanne, A. E. (2024). Modelling internal stem damage in savanna trees: Error in aboveground biomass with terrestrial laser scanning and allometry. *Methods in Ecology and Evolution*, 15, 1639–1652. <https://doi.org/10.1111/2041-210X.14375>